ACS OMEGA

http://pubs.acs.org/journal/acsodf

Article

Unconventional Type III Halogen···Halogen Interactions: A Quantum Mechanical Elucidation of σ-Hole···σ-Hole and Di-σ-Hole Interactions

Mahmoud A. A. Ibrahim* and Nayra A. M. Moussa

Cite This: *ACS Omega* 2020, 5, 21824−21835

Read Online

ACCESS | Metrics & More | Article Recommendations | Supporting Information

ABSTRACT: Herein, two unconventional type III halogen···halogen interactions, namely, σ-hole···σ-hole and di-σ-hole interactions, were reported in a series of halogenated complexes. In type III, the A-halogen···halogen angles are typically equal to 180°, and the occurrence of σ-hole on halogen atoms is mandatory. Using diverse quantum mechanical calculations, it was demonstrated that the occurrence of such interactions with binding energies varied from −0.35 to −1.30 kcal/mol. Symmetry-adapted perturbation theory-based energy decomposition analysis (SAPT-EDA) revealed that type III interactions are dominated by dispersion forces, while electrostatic forces are unfavorable. Cambridge Structure Database (CSD) survey unveiled the experimental evidence for the manifestation of σ-hole···σ-hole interactions in crystal structures. This work might be deemed as a foundation for a vast number of forthcoming crystal engineering and materials science studies.

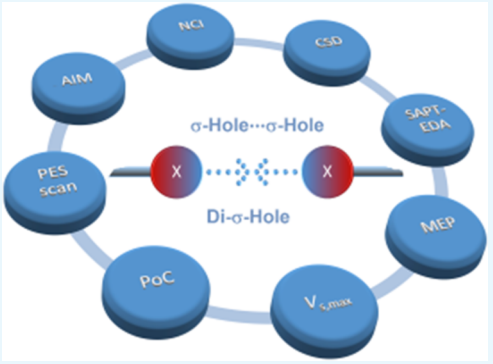

1. INTRODUCTION

Halogens are widely utilized to stabilize drug−protein[1] and supramolecular systems.[2,3] This is due to the ability of halogens to participate as Lewis bases and acids in noncovalent interactions with Lewis acids and bases, forming hydrogen[4] and halogen bonds,[5,6] respectively (Figure 1a). This dual behavior of halogens is mainly attributed to the anisotropic distribution of electron density around the halogen atom, forming a positive (or less negative) electrostatic potential along the A−X covalent bond (called σ-hole).[7−12] The ability of halogen-containing molecules to interact with Lewis acid/base at a halogen···Lewis acid/base angle of 180° has been reported.[13] In addition to hydrogen and halogen bonds, halogens participate in halogen···halogen inter- and intramolecular interactions, playing an important role in determining crystal packing and cohesion.[11,14,15] Characterization of halogen···halogen contacts has been a subject of a variety of theoretical and crystallographic studies.[9,16,17] According to the literature, halogen···halogen contacts can be classified into two main types: type I, in which the A-halogen···halogen angle (θ_1) is nearly equal to the halogen···halogen-A angle (θ_2) (Figure 1b), and type II, in which the θ_1 angle is about 180° and θ_2 is about 90° (Figure 1c).[16,18,19] Two different geometries could be taken for type I halogen···halogen contact, the cis- and trans-geometrical structures, as illustrated in Figure 1b. The interpretation of type I and II interactions can be given as a donor−acceptor interaction between an σ-hole on one halogen atom and a negative belt on the second halogen atom.[20] As mentioned earlier, the main force behind type I is van der Waals interaction, while the electrostatic force is the dominant factor in type II.[21,22]

Very recently, σ−σ-centered type II terminology has been proposed to describe fluorine-centered noncovalent interactions of atomic sites with positive or negative electrostatic potential.[23−25] So far, however, the ability of halogen-containing molecules to form type III halogen···halogen interaction, in which the θ_1 and θ_2 angles are typically equal to 180°, has not been yet well characterized. Consequently, the current study was designed to assess the versatility of halogen-containing molecules to form type III halogen···halogen interactions. The occurrence of positive σ-hole on both halogen atoms (i.e., A−X and A−X′) is a mandatory condition to characterize the halogen···halogen interaction with θ_1 and θ_2 angles of 180° as type III interaction. Based on the involved halogen-containing molecules, type III can be classified into (i) σ-hole···σ-hole (A−X···X−A) interaction, in which the halogen···halogen interaction occurs between two identically charged halogens, and (ii) di-σ-hole (A−X···X′−A) interaction, in which two different or not identically charged halogens are utilized.

In this study, geometrical optimization, molecular electrostatic potential (MEP), and maximum positive electrostatic potential ($V_{s,max}$) calculations will be carried out on halogen-containing molecules, namely, hydrogen halide (HX),

Received: June 16, 2020
Accepted: August 4, 2020
Published: August 19, 2020

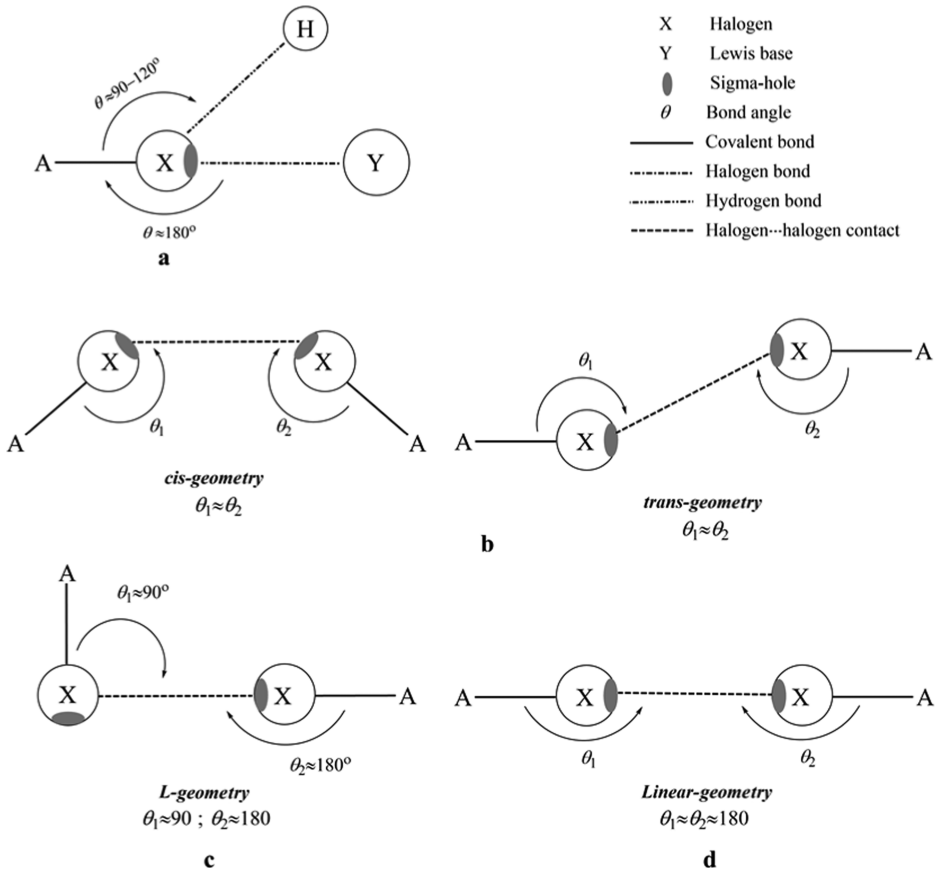

Figure 1. Schematic representation for (a) the dual behavior of the A−X molecule in noncovalent interactions, (b) cis- and trans-geometries of type I halogen···halogen interactions, (c) type II halogen···halogen interactions, and (d) type III halogen···halogen interactions.

halobenzene (C_6H_5X), and halomethane (CH_3X). With the help of the point-of-charge (PoC) approach, $^{\pm}\sigma$-hole tests will be executed to reveal the ability of investigated halomolecules to interact with both the Lewis base and acid from the electrostatic perspective. Moreover, potential energy surface (PES) scans will be performed for A−X···X/X′−A (where A = H, C_6H_5, and CH_3, and X/X′ = F, Cl, Br, and I) complexes. At the most favorable halogen···halogen distance, binding energies will be benchmarked at the CCSD(T)/CBS level of theory. Quantum theory of atoms in molecules (QTAIM), noncovalent interaction (NCI) index, and symmetry-adapted perturbation theory-based energy decomposition analysis (SAPT-EDA) will be established to explore the nature of the type III halogen···halogen interactions. Furthermore, a survey of the Cambridge Structure Database (CSD) will be conducted to explore the occurrence of such unconventional interactions in crystal structures. This study provides a solid characterization of the features and nature of type III halogen···halogen interactions, which will lead in turn to the enhancement of research in supramolecular chemistry and materials science.

2. RESULTS AND DISCUSSION

2.1. MEP, $V_{s,max}$, and $^{\pm}\sigma$-Hole Test. Molecular electrostatic potential (MEP) is a reliable method to conceive the electron-deficient and electron-rich regions on molecular systems, indicating the electrophilic and nucleophilic sites.[26,27] In this study, MEPs were generated for all of the optimized monomers at the MP2/aug-cc-pVTZ (with PP functions for Br and I atoms) level of theory and then mapped on 0.002 au electron density contours. MEP maps for all of the studied monomers are depicted in Figure 2.

According to MEP maps, σ-hole was observed along the extension of the A−X covalent bond on the molecular surface of halogen atoms in all studied halomolecules except in the fluorine-containing molecules. This exception might be attributed to the small size of the fluorine atom and its high electronegativity. Furthermore, the size of σ-hole increased with increasing atomic size of the halogen atom in the order Cl < Br < I.[28,29]

For computing the numerical value of σ-hole, the maximum positive electrostatic potential ($V_{s,max}$) calculations were carried out on the optimized monomers. The values of $V_{s,max}$ for all halomolecules are given in Figure 2. According to the $V_{s,max}$ results, the magnitude of σ-hole decreased as the electronegativity of the halogen atom increased to become negative in the case of fluorine-containing molecules. For the studied halomolecules, $V_{s,max}$ increased in the order halomethane < halobenzene < hydrogen halide. For instance, $V_{s,max}$ values of 21.0, 24.1, and 30.8 kcal/mol were obtained for iodomethane, iodobenzene, and hydrogen iodide, respectively.

It is worth noting that the absence of positive σ-hole on the investigated fluorine-containing molecules indicates their inability to form type III interactions, as discussed in the Section 1. As a result, all fluorine-centered interactions will be characterized as traditional halogen bonds between the negative fluorine atom and the positive σ-hole on the other halogen atom.

To assess the electrostatic potentiality of all studied halomolecules to participate in noncovalent interactions with

https://dx.doi.org/10.1021/acsomega.0c02887
ACS Omega 2020, 5, 21824−21835

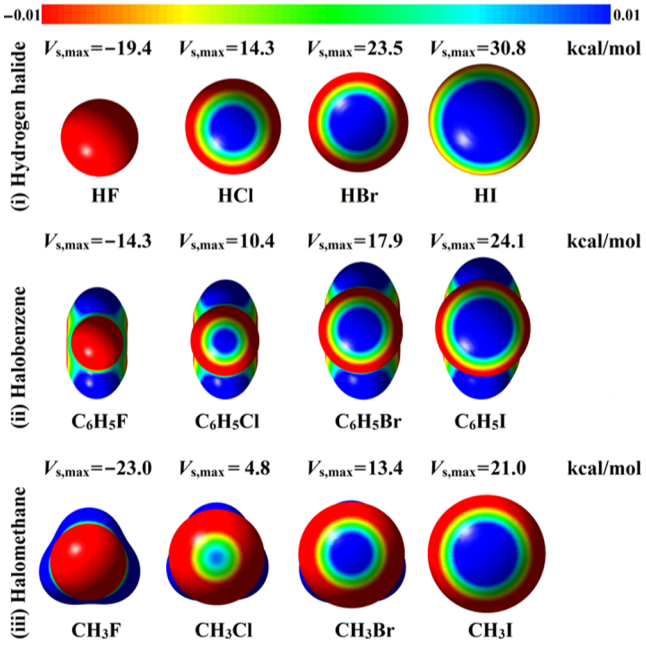

Figure 2. Molecular electrostatic potential (MEP) maps of hydrogen halide (HX), halobenzene (C_6H_5X), and halomethane (CH_3X) molecules plotted on to 0.002 au electron density contours. The electrostatic potential varies from −0.01 (red) to +0.01 (blue) au. The calculated maximum positive electrostatic potentials ($V_{s,max}$) of the studied molecules are given in kcal/mol.

Lewis base and acid at an A−X···base/acid angle of 180°, $^{-}\sigma$-hole and $^{+}\sigma$-hole tests were performed, respectively. The correlation between molecular stabilization energy and X··· PoC distance was studied in the range from 2.5 to 7.5 Å along the *x*-axis with a step size of 0.1 Å (Figure 3). Molecular stabilization energies of the A−X···PoC systems calculated in the presence of ±0.25 and ±0.75 au PoCs at an X···PoC distance of 2.5 Å with an A−X···PoC angle (θ) of 180° are compiled in Table 1.

According to the results of the $^{-}\sigma$-hole test, molecular stabilization energies were observed for all studied halomolecules in the presence of negative PoC with an exception for fluorine-containing molecules due to the absence of σ-hole (see the MEP maps in Figure 2). Furthermore, the molecular stabilization energy decreased as the X···PoC distance increased and the electronegativity of the halogen atom increased. For instance, molecular stabilization energies of HI···, HBr···, and HCl···PoC systems with a PoC value of −0.25 au at the X···PoC distance of 2.5 Å were found to be −4.61, −2.42, and −0.87 kcal/mol, respectively. Moreover, increasing the negativity of PoC value (i.e., Lewis basicity) enhanced the molecular stabilization energies of the A−X··· PoC systems. For instance, the presence of PoC with values of −0.25 and −0.75 au for the CH_3I···PoC system at a distance of 2.5 Å led to molecular energies of −3.07 and −16.76 kcal/mol, respectively.

In the case of $^{+}\sigma$-hole test, almost all of the studied halomolecules were observed with substantial molecular stabilization energies, especially in the presence of +0.75 au PoC at short A−X···PoC distances (Figure 3). It is worth pointing out that molecular destabilization and stabilization energies for A−I···PoC systems were recorded in the presence of +0.25 and +0.75 au PoC values, respectively. For the CH_3I··· PoC system, for instance, the molecular energies were 0.13 and −10.69 kcal/mol for +0.25 and +0.75 au PoC values, respectively. This informative result ensured the prominent role of polarization in the case of large PoC, which is in great accordance with our previous work.[13] Overall, molecular stabilization energies for the studied halomolecules in the presence of positive PoC were found to be inversely correlated with $V_{s,max}$ values. For instance, molecular energies of HX··· PoC systems with $V_{s,max}$ values of −19.4, 14.3, 23.5, and 30.8 kcal/mol (for X = F, Cl, Br, and I, respectively) were found to be −10.54, −5.24, −3.49, and −2.76 kcal/mol, respectively, in the presence of PoC of +0.75 au at an X···PoC distance of 2.5 Å.

2.2. Potential Energy Surface (PES) Scan. Potential energy surface (PES) scan was invoked to reveal the ability of halogen-containing molecules to participate in σ-hole···σ-hole and di-σ-hole interactions. PES scan was performed for HX··· XH, C_6H_5X···XC_6H_5, and CH_3X···XCH_3 (where X = F, Cl, Br, and I) complexes at an X···X/X′ distance ranging from 2.5 to 7.5 Å in the *x*-direction with a step size of 0.1 Å. Binding energy curves were generated at the MP2/aug-cc-pVTZ(PP) level of theory and are depicted in Figure 4. Moreover, CCSD(T)/CBS binding energies were also computed for type III complexes at the most favorable X···X/X′ distances and are listed in Table 2.

It can be concluded from the data presented in Figure 4 that all investigated halomolecules (except fluorine-containing molecules) can favorably interact with "like" halomolecules via σ-hole···σ-hole type III interactions. The binding energies of σ-hole···σ-hole interactions decreased with decreasing atomic size of the halogen atom in the order A−I···I−A > A−Br···Br−A > A−Cl···Cl−A complexes and faded in the case of A−F···F−A complexes. For instance, the CCSD(T)/CBS binding energies of CH_3I···ICH_3, CH_3Br···$BrCH_3$, and CH_3Cl···$ClCH_3$ complexes were obtained to be −1.07, −0.68, and −0.35 kcal/mol, respectively. The inability of fluorine-containing molecules to participate in σ-hole···σ-hole type III interactions might be related to the absence of σ-hole on the fluorine atom and the large repulsive electrostatic interaction between the two isotropic negative fluorine atoms. Furthermore, halobenzene complexes were obviously observed with maximum binding energies followed by halomethane, then hydrogen halide complexes. For instance, CCSD(T)/CBS binding energies of C_6H_5I···IC_6H_5, CH_3I···ICH_3, and HI···IH complexes were found to be −1.30, −1.07, and −0.65 kcal/mol, respectively. Based on the inspection of the aforementioned results, the σ-hole···σ-hole interactions might be explained as a sum of (i) attractive electrostatic forces between the positive σ-hole of one halogen atom and the negative belt of the other halogen atom, (ii) repulsive electrostatic forces between the positive σ-holes of the two halogen atoms, (iii) repulsive electrostatic forces between the negative belts of the two halogen atoms, (iv) the van der Waals interactions between the two halogen atoms, and (v) polarization contribution of one halogen atom by the other halogen atom.

Turning to "unlike" complexes, all investigated halomolecules showed solid potentiality to favorably interact with "unlike" halomolecules with A−X···X′ and A−X′···X angles of 180°. According to the data summarized in Table 2, the most favorable binding energies were denoted in the case of HF··· XH complexes. The interpretation of the binding energies of "unlike" fluorine-containing complexes might be relevant to the highly attractive forces between the isotropic negative fluorine atom in one monomer and positive σ-hole on the

https://dx.doi.org/10.1021/acsomega.0c02887
ACS Omega 2020, 5, 21824−21835

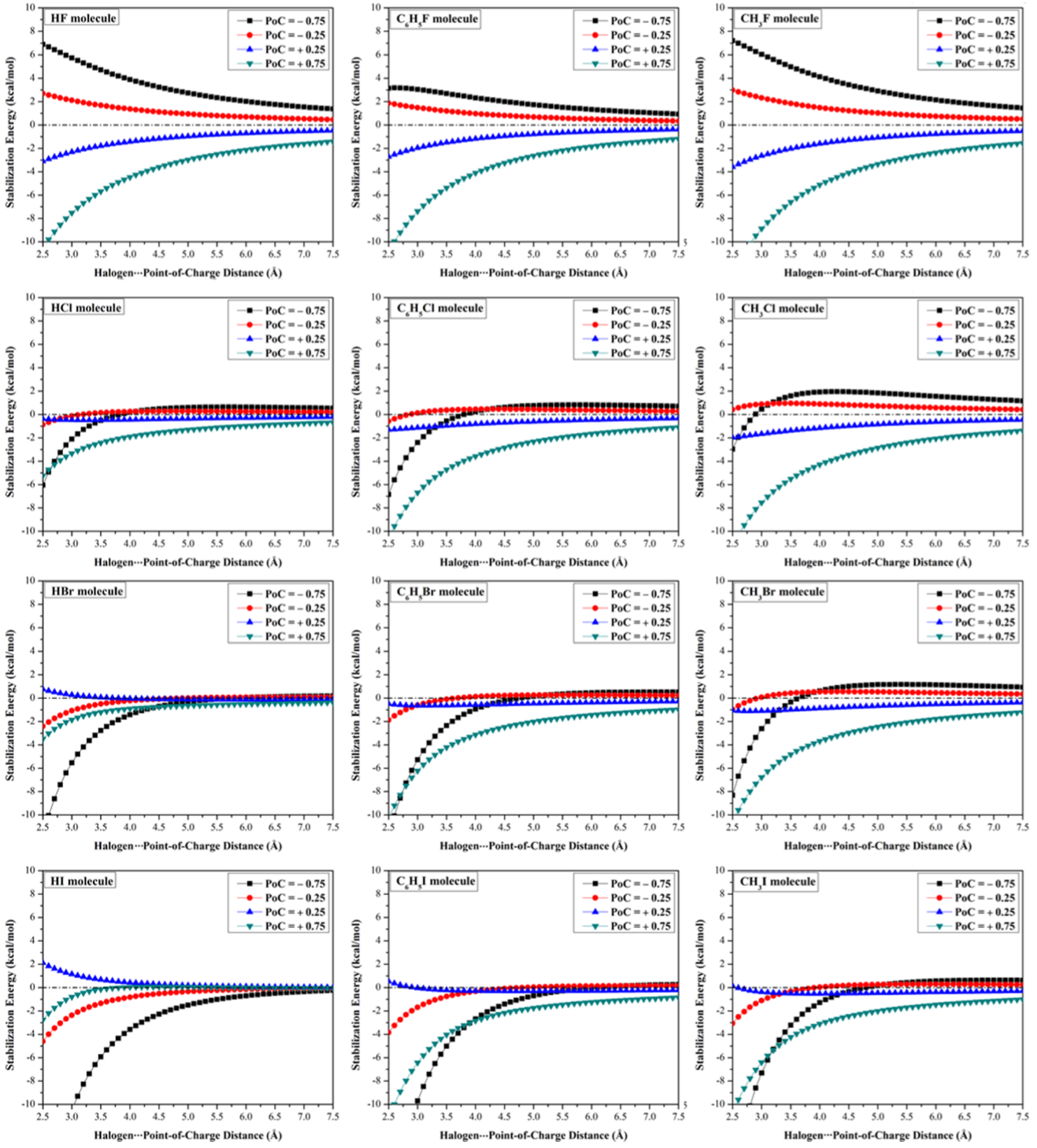

Figure 3. Molecular stabilization energies of the HX···, C_6H_5X···, and CH_3X···PoC systems in the presence of PoC with values of ±0.25 and ±0.75 au at the X···PoC distance ranging from 2.5 to 7.5 Å and the A−X···PoC angle (θ) of 180°.

"unlike" monomer. Consequently, the binding energy of the latter interaction increased as the σ-hole size of the "unlike" monomer increased in the order HF···ClH < HF···BrH < HF···IH with values of −0.37, −0.77, and −1.20 kcal/mol, respectively. Due to the lack of the σ-hole on the fluorine atom, the A−F···X′-A interaction might be characterized as a traditional halogen bond rather than di-σ-hole interaction.

For di-σ-hole interactions, the binding energies of the studied "unlike" complexes decreased in the order A−X···I−A > A−X···Br−A > A−X···Cl−A. For instance, the CCSD(T)/CBS binding energies were found to be −0.90, −0.68, and −0.55 kcal/mol for the CH_3Br···XCH_3 complexes, where X = I, Br, and Cl, respectively. This might reflect the favorable halogens' van der Waals contribution to the di-σ-hole binding energies.

To sum up, the aforesaid results endeavor to demonstrate the potentiality of the studied halomolecules (except fluorine-

https://dx.doi.org/10.1021/acsomega.0c02887
ACS Omega 2020, 5, 21824−21835

Table 1. Molecular Stabilization Energies of the A−X···PoC (Where A = H, C_6H_5, and CH_3X) Systems in the Presence of PoC with Values of ±0.25 and ±0.75 au at an X···PoC Distance of 2.5 Å and an A−X···PoC Angle of 180°

	molecular stabilization energy ($E_{stabilization}$, kcal/mol)							
	PoC = −0.25 au				PoC = −0.75 au			
molecule	F	Cl	Br	I	F	Cl	Br	I
HX	2.69	−0.87	−2.42	−4.61	6.90	−6.05	−11.78	−20.44
C_6H_5X	1.86	−0.58	−1.88	−3.85	3.15	−6.85	−11.93	−20.03
CH_3X	2.98	0.42	−0.97	−3.07	7.22	−2.97	−8.31	−16.76
	molecular stabilization energy ($E_{stabilization}$, kcal/mol)							
	PoC = +0.25 au				PoC = +0.75 au			
molecule	F	Cl	Br	I	F	Cl	Br	I
HX	−3.09	−0.37	0.76	2.11	−10.54	−5.24	−3.49	−2.76
C_6H_5X	−2.71	−1.30	−0.49	0.53	−10.83	−10.60	−10.25	−11.24
CH_3X	−3.58	−1.97	−1.06	0.13	−12.66	−11.29	−10.57	−10.69

containing molecules) to participate in σ-hole···σ-hole and di-σ-hole interactions.

2.3. QTAIM Analysis. Quantum theory of atoms in molecules (QTAIM) furnishes reliable information for the occurrence of noncovalent interactions through generating bond critical points (BCPs) and bond paths (BPs) between two interacting monomers.[30] In the present study, QTAIM calculations were accomplished for type III halogen···halogen complexes at the most favorable X···X/X′ distance at the MP2/aug-cc-pVTZ(PP) level of theory. Figure S1 presents the generated BCPs and BPs for all studied type III halogen···halogen complexes. The BCPs and BPs of halobenzene complexes, as an example, are displayed in Figure 5. Electron density (ρ_b), Laplacian ($\nabla^2\rho_b$), and total energy density (H_b) were also computed and are summarized in Table 3.

As shown in Figure 5, halobenzene complexes had one BCP and one BP between the two interacting monomers, which consistently emphasized the existence of σ-hole···σ-hole and di-σ-hole interactions. The same observation was denoted for all of the studied complexes depicted in Figure S1.

From Table 3, relatively low values of ρ_b and positive values of $\nabla^2\rho_b$ and H_b were observed, indicating the closed-shell nature of type III halogen···halogen interactions. In accordance with PES scan results (Table 2), there was a direct correlation between the H_b values at the BCP and the calculated binding energies of the considered complexes. For instance, the H_b values in $C_6H_5X\cdots XC_6H_5$ complexes were found to be 0.00592, 0.00556, and 0.00482 au with binding energies of −1.30, −0.95, and −0.71 kcal/mol for X = I, Br, and Cl, respectively.

2.4. NCI Analysis. Toward a deeper understanding of the nature of σ-hole···σ-hole and di-σ-hole interactions, the noncovalent interaction (NCI) index was executed for type III halogen···halogen complexes at the most favorable X···X/X′ distances. Through NCI analysis, the two-dimensional (2D) reduced density gradient (RDG) and the three-dimensional (3D) color-mapped plots of noncovalent interaction regions were generated and are depicted in Figures S2 and S3, respectively. Figure 6 shows the 3D color-mapped plots of the iodobenzene complexes as an example.

Subject to 2D plots of the studied halogen···halogen complexes, all of the spikes denoted with negative values of sign(λ_2)ρ confirm the attractive interactions between two interacting halogen-containing monomers. Also, a low gradient was apparently discriminated in the case of HX···XH interactions and then peaked in $CH_3X\cdots XCH_3$ and $C_6H_5X\cdots XC_6H_5$ interactions, reflecting the trend of the calculated binding energies (Figure S2).

Moreover, the expanded green regions between the two interacting monomers in Figure S3 were obviously denoted, indicating the occurrence of weak attractive interactions between the interacting monomers. From the inspection of QTAIM and NCI results, we can affirm the potentiality of the studied halomolecules to participate in σ-hole···σ-hole and di-σ-hole interactions that are in line with molecular stabilization and binding energies of similar patterns.

2.5. SAPT-EDA Calculation. Symmetry-adapted perturbation theory-based energy decomposition analysis (SAPT-EDA) is an adequate tool to scrutinize the nature of noncovalent interactions in molecular systems.[31] For the investigated type III halogen···halogen complexes, energy decomposition analysis was executed using the SAPT0 level of truncation. Table 4 gathers the total SAPT-based binding energy (E_{SAPT0}) and its basic contributing factors calculated in kcal/mol.

The total SAPT-based binding energy (E_{SAPT0}) for the studied complexes were similar to the BSSE-corrected MP2/aug-cc-PVTZ(PP) binding energies (ΔΔE was close to 0 kcal/mol, Table 4), demonstrating the reliability of the implemented SAPT level of theory.

The SAPT-EDA results given in Table 4 revealed that type III halogen···halogen interactions were dominated by dispersion forces (E_{disp}). These results demonstrated that the nature of type III halogen···halogen interactions is similar to that of type I halogen···halogen interactions. In contrast to type II halogen···halogen interactions, the electrostatic forces (E_{elst}) were repulsive in the case of σ-hole···σ-hole and di-σ-hole interactions and attractive in the case of traditional halogen bond (i.e., in fluorine-containing complexes). The positive E_{elst} values were expected as a result of repulsion between the interacting sites of similar electrostatic potential (i.e., the two positive σ-holes and the two negative belts of halogen atoms). The larger the σ-hole size, the more unfavorable the E_{elst} contribution, becoming attractive when σ-hole is absent. For example, the E_{elst} of the $CH_3I\cdots ICH_3$, $CH_3I\cdots BrCH_3$, $CH_3I\cdots ClCH_3$, and $CH_3I\cdots FCH_3$ complexes were observed with values of 0.25, 0.18, 0.01, and −0.92 kcal/mol, respectively, where σ-hole size decreased in the same order: I > Br > Cl and disappeared in F. The exchange repulsion (E_{exch}) and induction (E_{ind}) components were positive and negative for all studied complexes, respectively.

Overall, the SAPT-EDA results of type III halogen···halogen interactions exhibited a prominent similarity in dispersive

https://dx.doi.org/10.1021/acsomega.0c02887
ACS Omega 2020, 5, 21824−21835

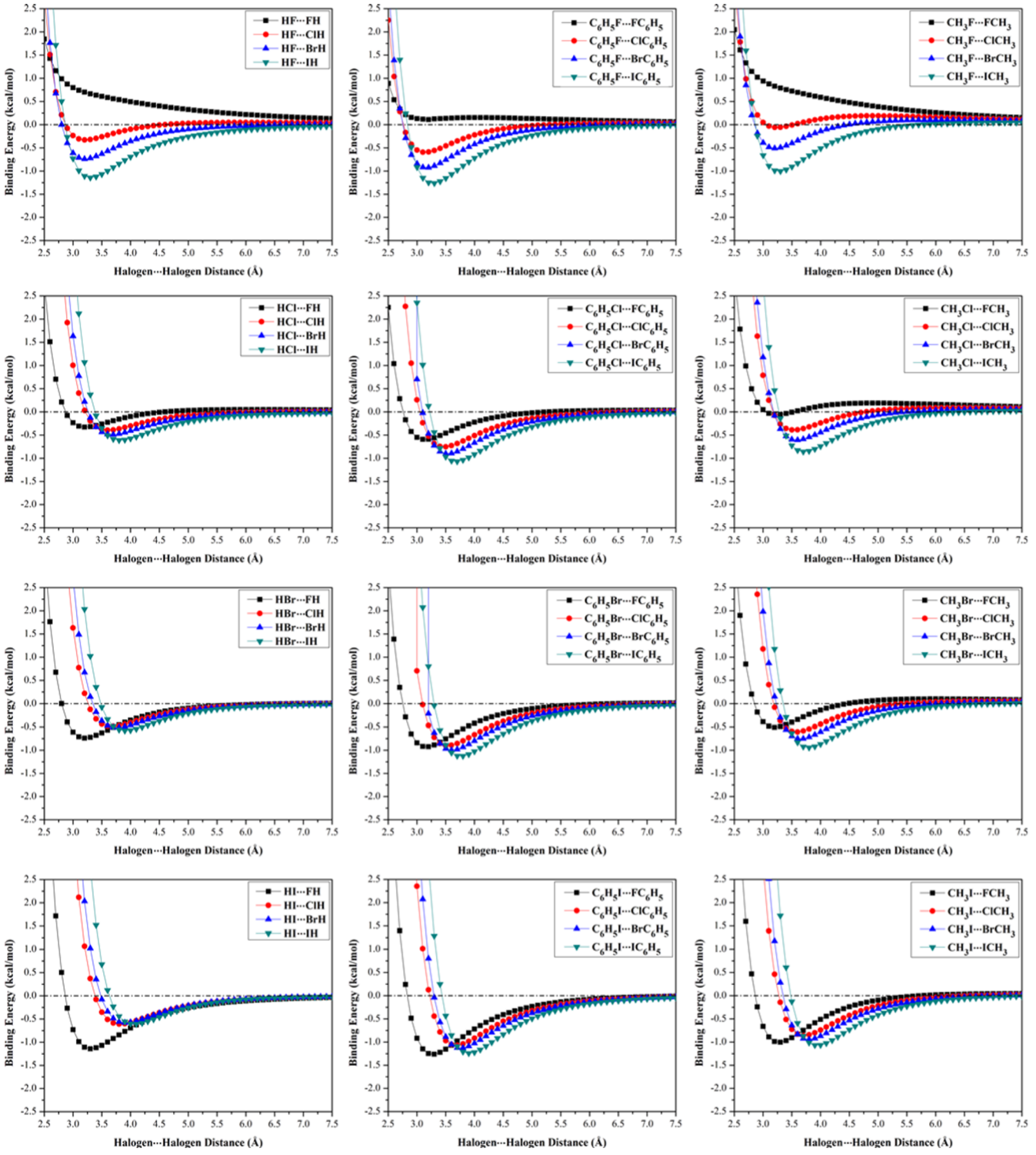

Figure 4. Potential energy surface (PES) curves for HX···XH, $C_6H_5X···XC_6H_5$, and $CH_3X···XCH_3$ (where X = F, Cl, Br, and I) complexes calculated (in kcal/mol) at the MP2/aug-cc-pVTZ(PP) level of theory at an X···X/X′ distance ranging from 2.5 to 7.5 Å and with an A−X···X/X′ angle (θ) of 180°.

nature with the analogues of type I interactions. Unlike type I interactions, electrostatic forces in type III halogen···halogen interactions were unfavorable.

2.6. CSD Survey. To pinpoint the reliability of type III halogen···halogen interactions, the CSD database was explored to investigate the existence of such interactions in the solid state. The CSD survey unveiled 24 crystal structures with the standard geometric requirements for desired type III interactions (see the Section 4 for details). The CSD codes, halogen···halogen distances, and A-halogen···halogen angles (θ) of the identified hits are collected in Table S1. It can be seen from the data in Table S1 that the halogen···halogen distances in identified crystal structures are smaller than the sum of van der Waals radii of the contacted halogen atoms.

https://dx.doi.org/10.1021/acsomega.0c02887
ACS Omega 2020, 5, 21824−21835

Table 2. Binding Energies Calculated (in kcal/mol) at the MP2/aug-cc-pVTZ(PP) and CCSD(T)/CBS Levels of Theories for HX···XH, C_6H_5X···XC_6H_5, and CH_3X···XCH_3 (Where X = F, Cl, Br, and I) Complexes at the Most Favorable X···X/X′ Distances

complexes		σ-hole binding features			
		interaction type	distance (Å)	$E_{MP2/aug\text{-}cc\text{-}pVTZ(PP)}$ (kcal/mol)	$E_{CCSD(T)/CBS}$ (kcal/mol)
hydrogen halide	HI···IH	σ-hole···σ-hole	4.06	−0.61	−0.65
	HI···BrH	di-σ-hole	3.91	−0.58	−0.56
	HI···ClH	di-σ-hole	3.82	−0.61	−0.56
	HI···FH	halogen bond	3.30	−1.14	−1.20
	HBr···BrH	σ-hole···σ-hole	3.76	−0.51	−0.46
	HBr···ClH	di-σ-hole	3.69	−0.49	−0.44
	HBr···FH	halogen bond	3.20	−0.74	−0.77
	HCl···ClH	σ-hole···σ-hole	3.61	−0.39	−0.35
	HCl···FH	halogen bond	3.21	−0.33	−0.37
	HF···FH	repulsive	[a]	[a]	[a]
halobenzene	C_6H_5I···IC_6H_5	σ-hole···σ-hole	3.90	−1.23	−1.30
	C_6H_5I···BrC_6H_5	di-σ-hole	3.75	−1.13	−1.13
	C_6H_5I···ClC_6H_5	di-σ-hole	3.68	−1.07	−1.06
	C_6H_5I···FC_6H_5	halogen bond	3.27	−1.26	−1.21
	C_6H_5Br···BrC_6H_5	σ-hole···σ-hole	3.61	−1.00	−0.95
	C_6H_5Br···ClC_6H_5	di-σ-hole	3.53	−0.90	−0.85
	C_6H_5Br···FC_6H_5	halogen bond	3.16	−0.93	−0.93
	C_6H_5Cl···ClC_6H_5	σ-hole···σ-hole	3.47	−0.75	−0.71
	C_6H_5Cl···FC_6H_5	halogen bond	3.14	−0.60	−0.59
	C_6H_5F···FC_6H_5	repulsive	[a]	[a]	[a]
halomethane	CH_3I···ICH_3	σ-hole···σ-hole	3.94	−1.07	−1.07
	CH_3I···$BrCH_3$	di-σ-hole	3.79	−0.94	−0.90
	CH_3I···$ClCH_3$	di-σ-hole	3.71	−0.86	−0.81
	CH_3I···FCH_3	halogen bond	3.28	−1.01	−1.00
	CH_3Br···$BrCH_3$	σ-hole···σ-hole	3.65	−0.76	−0.68
	CH_3Br···$ClCH_3$	di-σ-hole	3.58	−0.61	−0.55
	CH_3Br···FCH_3	halogen bond	3.20	−0.51	−0.52
	CH_3Cl···$ClCH_3$	σ-hole···σ-hole	3.54	−0.39	−0.35
	CH_3Cl···FCH_3	halogen bond	3.23	−0.06	−0.08
	CH_3F···FCH_3	repulsive	[a]	[a]	[a]

[a]No local minimum was observed in the corresponding potential energy surface (PES) curves for A−F···F−A complexes (Figure 4).

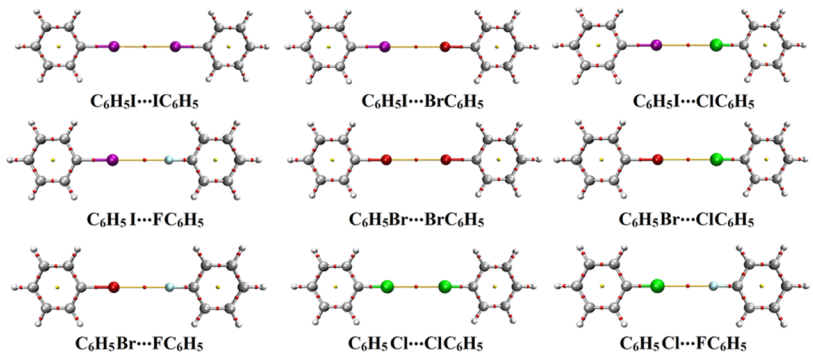

Figure 5. Quantum theory of atoms in molecules (QTAIM) diagrams for C_6H_5X···XC_6H_5 (where X = F, Cl, Br, and I) complexes at the most favorable X···X/X′ distances. The red dots indicate the locations of bond critical points (BCP) at bond paths (BP) between two interacting monomers.

Interestingly, investigation of the hits revealed that all observed type III interactions are σ-hole···σ-hole (see Table S1). The absence of di-σ-hole interactions in the explored hits emphasized the relatively low strength of such interactions compared to those of σ-hole···σ-hole interactions. These results are in line with the calculated binding energies, which showed the favorability of the inspected halomolecules to participate in σ-hole···σ-hole interactions rather than di-σ-hole interactions (see Table 2). Three crystal structures demonstrating σ-hole···σ-hole interactions are given in Figure 7.

As shown in Figure 7, I···I interactions are established in AYURES between two directional and identical iodine-containing molecules, which emphasizes the occurrence of σ-hole···σ-hole interaction. Such interaction was also denoted between identical bromine- and chlorine-containing molecules in TPHMBR02 and ZZZVTY12, respectively. Overall, it is

https://dx.doi.org/10.1021/acsomega.0c02887
ACS Omega 2020, 5, 21824−21835

Table 3. Topological Parameters Including Electron Density (ρ_b, au), Laplacian ($\nabla^2\rho_b$, au), and Total Energy Density (H_b, au) at Bond Critical Points (BCPs) of HX···XH, C_6H_5X···XC_6H_5, and CH_3X···XCH_3 (Where X = F, Cl, Br, and I) Complexes at the Most Favorable X···X/X′ Distances

complexes		interaction type	ρ_b (au)	$\nabla^2\rho_b$ (au)	H_b (au)
hydrogen halide	HI···IH	σ-hole···σ-hole	0.00076	0.01383	0.00404
	HI···BrH	di-σ-hole	0.00086	0.01484	0.00389
	HI···ClH	di-σ-hole	0.00093	0.01531	0.00381
	HI···FH	halogen bond	0.00130	0.02619	0.00578
	HBr···BrH	σ-hole···σ-hole	0.00097	0.01593	0.00376
	HBr···ClH	di-σ-hole	0.00101	0.01577	0.00354
	HBr···FH	halogen bond	0.00138	0.02582	0.00517
	HCl···ClH	σ-hole···σ-hole	0.00107	0.01593	0.00341
	HCl···FH	halogen bond	0.00128	0.02154	0.00408
	HF···FH	repulsive	[a]	[a]	[a]
halobenzene	C_6H_5I···IC_6H_5	σ-hole···σ-hole	0.00078	0.01818	0.00592
	C_6H_5I···BrC_6H_5	di-σ-hole	0.00093	0.01991	0.00578
	C_6H_5I···ClC_6H_5	di-σ-hole	0.00105	0.02011	0.00542
	C_6H_5I···FC_6H_5	halogen bond	0.00129	0.0279	0.00643
	C_6H_5Br···BrC_6H_5	σ-hole···σ-hole	0.00107	0.02135	0.00556
	C_6H_5Br···ClC_6H_5	di-σ-hole	0.00128	0.02225	0.00530
	C_6H_5Br···FC_6H_5	halogen bond	0.00140	0.02827	0.00593
	C_6H_5Cl···ClC_6H_5	σ-hole···σ-hole	0.00144	0.02217	0.00482
	C_6H_5Cl···FC_6H_5	halogen bond	0.00145	0.02564	0.00501
	C_6H_5F···FC_6H_5	repulsive	[a]	[a]	[a]
halomethane	CH_3I···ICH_3	σ-hole···σ-hole	0.00074	0.01686	0.00549
	CH_3I···$BrCH_3$	di-σ-hole	0.00087	0.01838	0.00534
	CH_3I···$ClCH_3$	di-σ-hole	0.00102	0.01903	0.00509
	CH_3I···FCH_3	halogen bond	0.00129	0.02762	0.00631
	CH_3Br···$BrCH_3$	σ-hole···σ-hole	0.00100	0.01959	0.00513
	CH_3Br···$ClCH_3$	di-σ-hole	0.00113	0.01986	0.00480
	CH_3Br···FCH_3	halogen bond	0.00133	0.02615	0.00544
	CH_3Cl···$ClCH_3$	σ-hole···σ-hole	0.00117	0.01870	0.00422
	CH_3Cl···FCH_3	halogen bond	0.00121	0.02084	0.00412
	CH_3F···FCH_3	repulsive	[a]	[a]	[a]

[a]No local minimum was observed in the corresponding potential energy surface (PES) curves for A−F···F−A complexes (Figure 4).

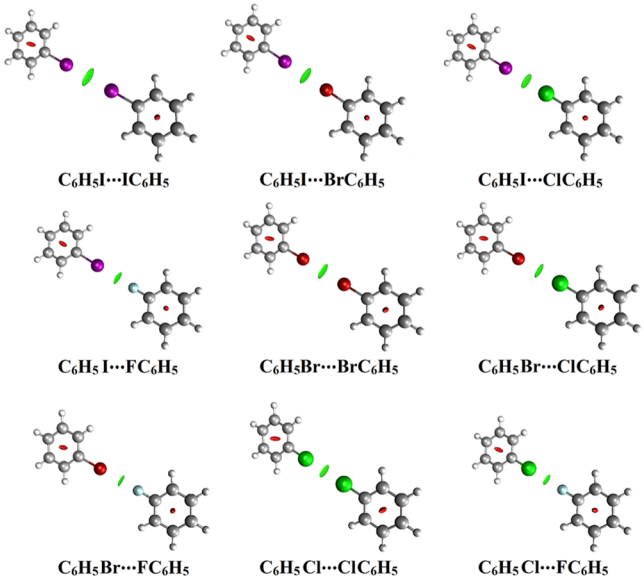

Figure 6. 3D NCI plots of C_6H_5I···XC_6H_5 (where X = F, Cl, Br, and I) complexes at the most favorable X···X/X′ distance. The isosurfaces are plotted with a reduced density gradient value of 0.50 au and colored from blue to red according to sign(λ_2)ρ ranging from −0.035 (blue) to 0.020 (red) au.

appealing to affirm the versatility of halomolecules to engage in type III halogen···halogen interactions.

3. CONCLUSIONS

This study has proved the occurrence of σ-hole···σ-hole and di-σ-hole interactions in a series of halogenated complexes in which the halogen···halogen interaction observed between two identically charged halogens and two different ones, respectively. Substantial binding energies were denoted for all of the studied halomolecules, interpreted as the sum of (i) attractive electrostatic forces between the positive σ-hole of one halogen atom and the negative belt of the other halogen atom, (ii) repulsive electrostatic forces between the positive σ-holes of the two halogen atoms, (iii) repulsive electrostatic forces between the negative belts of the two halogen atoms, (iv) the van der Waal interactions between the two halogen atoms, and (v) polarization contribution of one halogen atom by the other halogen atom. Fluorine-based interactions were recognized as traditional halogen bonds, due to the absence of σ-hole on the fluorine atom. The closed-shell nature of type III halogen···halogen interactions was elucidated through the incorporation of the quantum theory of atoms in molecules (QTAIM) and noncovalent interaction (NCI) index calculations. Symmetry-adapted perturbation theory-based energy decomposition analysis (SAPT-EDA) revealed that dispersion energy plays a crucial role in the σ-hole···σ-hole and di-σ-hole

https://dx.doi.org/10.1021/acsomega.0c02887
ACS Omega 2020, 5, 21824−21835

Table 4. Symmetry-Adapted Perturbation Theory-Based Energy Decomposition Analysis (SAPT-EDA) for HX···XH, C_6H_5X···XC_6H_5, and CH_3X···XCH_3 (Where X = F, Cl, Br, and I) Complexes Calculated (in kcal/mol) at the MP2/aug-cc-pVTZ(PP) Level of Theory and the Most Favorable X···X/X′ Distances

complexes		interaction type	$E_{elst}^{(10)}$	$E_{exch}^{(10)}$	E_{disp}	E_{ind}	E_{SAPT0} [a]	$\Delta\Delta E$ [b]
hydrogen halide	HI···IH	σ-hole···σ-hole	0.66	1.02	−1.91	−0.29	−0.52	−0.09
	HI···BrH	di-σ-hole	0.44	0.86	−1.62	−0.20	−0.53	−0.05
	HI···ClH	di-σ-hole	0.16	0.80	−1.41	−0.15	−0.61	0.00
	HI···FH	halogen bond	−1.32	1.22	−1.10	−0.31	−1.50	0.36
	HBr···BrH	σ-hole···σ-hole	0.33	0.72	−1.40	−0.14	−0.48	−0.03
	HBr···ClH	di-σ-hole	0.18	0.62	−1.18	−0.10	−0.48	−0.01
	HBr···FH	halogen bond	−0.70	0.86	−0.90	−0.20	−0.94	0.20
	HCl···ClH	σ-hole···σ-hole	0.15	0.54	−1.02	−0.07	−0.39	0.00
	HCl···FH	halogen bond	−0.15	0.53	−0.67	−0.11	−0.41	0.08
	HF···FH	repulsive	[c]	[c]	[c]	[c]	[c]	[c]
halobenzene	C_6H_5I···IC_6H_5	σ-hole···σ-hole	0.40	1.92	−2.98	−0.47	−1.12	−0.11
	C_6H_5I···BrC_6H_5	di-σ-hole	0.25	1.66	−2.64	−0.35	−1.08	−0.05
	C_6H_5I···ClC_6H_5	di-σ-hole	0.03	1.46	−2.30	−0.28	−1.08	0.01
	C_6H_5I···FC_6H_5	halogen bond	−0.99	1.51	−1.80	−0.33	−1.62	0.36
	C_6H_5Br···BrC_6H_5	σ-hole···σ-hole	0.21	1.39	−2.31	−0.25	−0.96	−0.04
	C_6H_5Br···ClC_6H_5	di-σ-hole	0.11	1.25	−2.05	-0.20	−0.89	−0.01
	C_6H_5Br···FC_6H_5	halogen bond	−0.46	1.12	−1.53	−0.22	−1.09	0.16
	C_6H_5Cl···ClC_6H_5	σ-hole···σ-hole	0.13	1.03	−1.76	−0.15	−0.75	0.00
	C_6H_5Cl···FC_6H_5	halogen bond	−0.04	0.77	−1.24	−0.15	−0.65	0.05
	C_6H_5F···FC_6H_5	repulsive	[c]	[c]	[c]	[c]	[c]	[c]
halomethane	CH_3I···ICH_3	σ-hole···σ-hole	0.25	1.82	−2.69	−0.39	−1.02	−0.05
	CH_3I···$BrCH_3$	di-σ-hole	0.18	1.57	−2.36	−0.31	−0.91	−0.03
	CH_3I···$ClCH_3$	di-σ-hole	0.01	1.43	−2.04	−0.26	−0.85	−0.01
	CH_3I···FCH_3	halogen bond	−0.92	1.57	−1.48	−0.41	−1.24	0.23
	CH_3Br···$BrCH_3$	σ-hole···σ-hole	0.24	1.31	−2.04	−0.22	−0.70	−0.06
	CH_3Br···$ClCH_3$	di-σ-hole	0.22	1.14	−1.74	−0.18	−0.56	−0.05
	CH_3Br···FCH_3	halogen bond	−0.14	1.05	−1.19	−0.27	−0.54	0.03
	CH_3Cl···$ClCH_3$	σ-hole···σ-hole	0.34	0.87	−1.41	−0.13	−0.33	−0.06
	CH_3Cl···FCH_3	halogen bond	0.44	0.59	−0.86	−0.17	0.01	−0.07
	CH_3F···FCH_3	repulsive	[c]	[c]	[c]	[c]	[c]	[c]

[a] $E_{SAPT0} = E_{elst}^{(10)} + E_{exch}^{(10)} + E_{disp} + E_{ind}$. [b] $\Delta\Delta E = E_{MP2/aug\text{-}cc\text{-}pVTZ(PP)} - E_{SAPT0}$. [c] No SAPT-EDA was performed since no local minimum was observed in the corresponding potential energy surface (PES) curves for A−F···F−A complexes (Figure 4).

interactions. However, the traditional halogen bond in the studied fluorine-containing complexes was stabilized by electrostatic forces. Through exploring the Cambridge Structure Database (CSD), several crystal structures were identified to reveal the experimental reliability of σ-hole···σ-hole interactions. Overall, these findings will enrich the role of halogen···halogen contacts in crystal engineering and materials design.

4. COMPUTATIONAL METHODOLOGY

In the current study, the ability of hydrogen halide (HX), halobenzene (C_6H_5X), and halomethane (CH_3X) (where X = F, Cl, Br, and I) to participate in type III halogen···halogen interactions was investigated. Initially, geometrical structures of the monomers were fully optimized by the second-order Møller−Plesset (MP2) method[32] with the aug-cc-pVTZ-PP basis set[33−35] for the Br and I atoms and the aug-cc-pVTZ basis set[33,34] for all other atoms. On the optimized structures, molecular electrostatic potentials (MEPs) were generated and mapped on 0.002 au electron density contours as previously recommended, where the 0.001 au isodensity envelope may provide incorrect information about the complete nature of the surface reactive sites.[23,36]

Moreover, maximum positive electrostatic potential ($V_{s,max}$) values were also computed using Multiwfn 3.5 software.[37] To reveal the halogens' interactions from the electrostatic perspective, $^{\pm}\sigma$-hole tests were carried out for the studied monomers with the point-of-charge (PoC) approach.[13,38−43] In the PoC approach, negative and positive PoCs were used to mimic Lewis bases and acids in $^{-}\sigma$-hole and $^{+}\sigma$-hole tests, respectively. Through $^{\pm}\sigma$-hole tests, the effect of the X···PoC distance on the molecular stabilization energy was examined in the range 2.5−7.5 Å along the *x*-axis with a step size of 0.1 Å and A−X···PoC angle (θ) of 180°. The molecular stabilization energies ($E_{stabilization}$) were computed in the presence of PoC with values of ±0.25 and ±0.75 au, and are estimated as follows

$$E_{stablization} = E_{halomolecule\cdots PoC} - E_{halomolecule}$$

The PoC values of ±0.25 and ±0.75 au were selected to represent moderate Lewis basicity and acidity. In the current study, the optimized structures of the monomers were kept frozen and placed relatively in one plane to form type III halogen···halogen interactions (i.e., with A−X···X/X′ angle of 180°, see Figure 1d). Potential energy surface (PES) scan was then performed at X···X/X′ distances from 2.5 to 7.5 Å in the *x*-direction with a step size of 0.1 Å, and the corresponding binding energy curves were generated. Binding energy was estimated as the difference between the energy of the complex and the sum of energies of the monomers. The basis set

https://dx.doi.org/10.1021/acsomega.0c02887
ACS Omega 2020, 5, 21824−21835

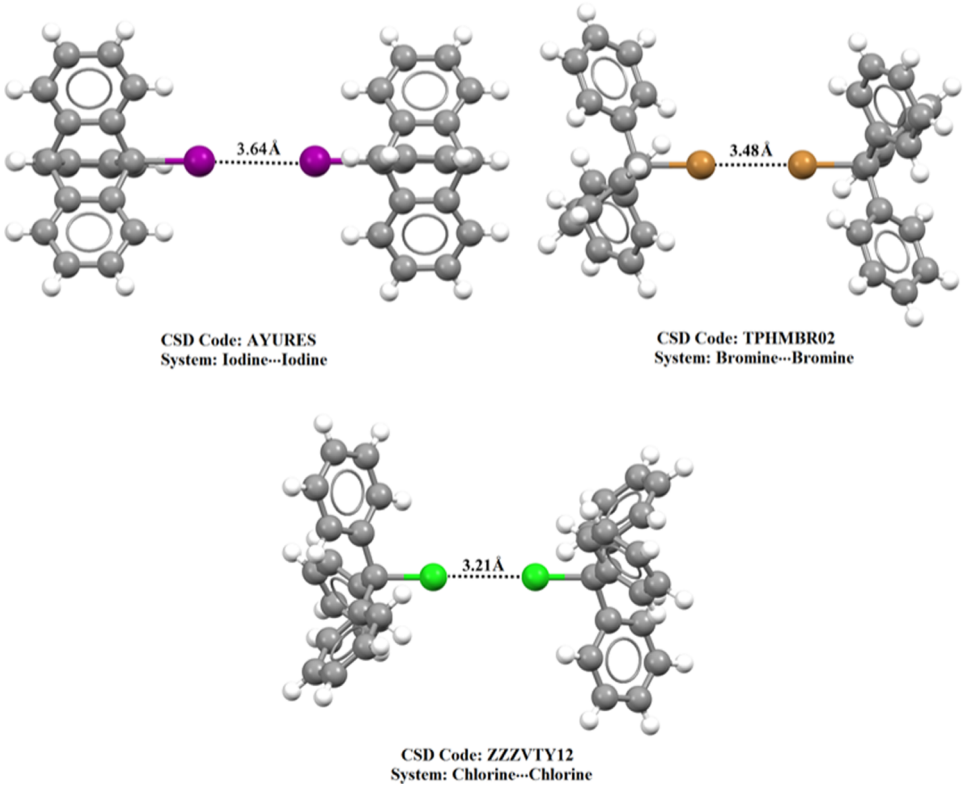

Figure 7. Type III halogen···halogen interactions in crystal structures.

superposition error (BSSE) was taken into account using the counterpoise correction method.[44] Also, CCSD(T)/CBS binding energies were estimated for the studied complexes at the most favorable X···X/X′ distances using the following equations[45]

$$E_{\mathrm{CCSD(T)/CBS}} = \Delta E_{\mathrm{MP2/CBS}} + \Delta E_{\mathrm{CCSD(T)}}$$

where

$$\Delta E_{\mathrm{MP2/CBS}} = (64E_{\mathrm{MP2/aug-cc-pVQZ}} - 27E_{\mathrm{MP2/aug-cc-pVTZ}})/37$$

$$\Delta E_{\mathrm{CCSD(T)}} = E_{\mathrm{CCSD(T)/aug-cc-pVdZ}} - E_{\mathrm{MP2/aug-cc-pVDZ}}$$

Moreover, the occurrence of type III halogen···halogen interaction in the studied complexes was unveiled through the incorporation of the quantum theory of atoms in molecules (QTAIM).[30] For type III complexes at the most favorable X···X/X′ distances, bond critical points (BCPs) and bond paths (PBs) were generated and visualized. The topological features including electron density (ρ_b), Laplacian density ($\nabla^2\rho_b$), and total energy density (H_b) were investigated. The noncovalent interaction (NCI) index was also established and NCI plots were depicted.[46]

To set forth the physical nature of the type III halogen···halogen interactions, symmetry-adapted perturbation theory-based energy decomposition analysis (SAPT-EDA) was performed at the SAPT0 level of truncation[47,48] using PSI4 code.[49] In the context of SAPT-EDA, total binding energy was estimated as the sum of its basic physical components, namely, electrostatic ($E_{\mathrm{elst}}^{(10)}$), exchange ($E_{\mathrm{exch}}^{(10)}$), dispersion (E_{disp}), and induction (E_{ind}), as follows

$$E_{\mathrm{SAPT0}} = E_{\mathrm{elst}}^{(10)} + E_{\mathrm{exch}}^{(10)} + E_{\mathrm{disp}} + E_{\mathrm{ind}}$$

where

$$E_{\mathrm{disp}} = E_{\mathrm{disp}}^{(20)} + E_{\mathrm{exch-disp}}^{(20)}$$

$$E_{\mathrm{ind}} = E_{\mathrm{ind.resp}}^{(20)} + E_{\mathrm{exch-ind.resp}}^{(20)} + \delta_{\mathrm{HF}}^{(2)}$$

All quantum mechanical calculations were performed using Gaussian09 software[50] at the same level of the theory of geometrical optimization. Besides, QTAIM and NCI analyses were implemented using Multiwfn 3.5 software.[37] QTAIM and NCI plots were visualized using Visual Molecular Dynamics (VMD) software.[51]

Finally, the Cambridge Structure Database (CSD version 5.41,[52,53] updated in November 2019) survey was executed to explore the occurrence of σ-hole···σ-hole and di-σ-hole type III interactions in crystal structures. The survey was limited to consider only chlorlo-, bromo-, and iodo-hydrocarbons (i.e., C−X···X−C and C−X···X′−C, where X = Cl, Br, and I). Fluorine-containing molecules were excluded from the survey to avoid contamination of the results by the traditional halogen-bonded complexes. The halogen···halogen angles (i.e., C−X···X′ and C−X′···X) were explored in the range of 179−180°. The halogen···halogen contact parameters and angles were defined using the "3D" function of Conquest.

■ ASSOCIATED CONTENT

Supporting Information

The Supporting Information is available free of charge at https://pubs.acs.org/doi/10.1021/acsomega.0c02887.

Quantum theory of atoms in molecules (QTAIM) diagrams, 2D noncovalent interaction (NCI) reduced

https://dx.doi.org/10.1021/acsomega.0c02887
ACS Omega 2020, 5, 21824−21835

density gradient (RDG) plots, 3D noncovalent interaction (NCI) plots for the studied halogen···halogen complexes; and a list of hits resulted from CSD survey (PDF)

AUTHOR INFORMATION

Corresponding Author

Mahmoud A. A. Ibrahim − *Computational Chemistry Laboratory, Chemistry Department, Faculty of Science, Minia University, Minia 61519, Egypt;* orcid.org/0000-0003-4819-2040; Email: m.ibrahim@compchem.net

Author

Nayra A. M. Moussa − *Computational Chemistry Laboratory, Chemistry Department, Faculty of Science, Minia University, Minia 61519, Egypt;* orcid.org/0000-0003-3712-7710

Complete contact information is available at: https://pubs.acs.org/10.1021/acsomega.0c02887

Notes

The authors declare no competing financial interest.

ACKNOWLEDGMENTS

The computational work was completed with resources supported by the Science and Technology Development Fund, STDF, Egypt, grant nos. 5480 and 7972.

REFERENCES

(1) Sirimulla, S.; Bailey, J. B.; Vegesna, R.; Narayan, M. Halogen interactions in protein-ligand complexes: implications of halogen bonding for rational drug design. *J. Chem. Inf. Model.* **2013**, *53*, 2781−2791.

(2) Priimagi, A.; Cavallo, G.; Metrangolo, P.; Resnati, G. The halogen bond in the design of functional supramolecular materials: recent advances. *Acc. Chem. Res.* **2013**, *46*, 2686−2695.

(3) Metrangolo, P.; Meyer, F.; Pilati, T.; Resnati, G.; Terraneo, G. Halogen bonding in supramolecular chemistry. *Angew. Chem., Int. Ed.* **2008**, *47*, 6114−6127.

(4) Brammer, L.; Bruton, E. A.; Sherwood, P. Understanding the behavior of halogens as hydrogen bond acceptors. *Cryst. Growth Des.* **2001**, *1*, 277−290.

(5) Cavallo, G.; Metrangolo, P.; Milani, R.; Pilati, T.; Priimagi, A.; Resnati, G.; Terraneo, G. The Halogen Bond. *Chem. Rev.* **2016**, *116*, 2478−2601.

(6) Feng, G.; Evangelisti, L.; Gasparini, N.; Caminati, W. On the Cl...N halogen bond: a rotational study of CF3Cl···NH3. *Chem. − Eur. J.* **2012**, *18*, 1364−1368.

(7) Clark, T.; Hennemann, M.; Murray, J. S.; Politzer, P. Halogen bonding: the σ-hole. *J. Mol. Model.* **2007**, *13*, 291−296.

(8) Varadwaj, A.; Varadwaj, P. R.; Jin, B. Y. Can an entirely negative fluorine in a molecule, viz. perfluorobenzene, interact attractively with the entirely negative site(s) on another molecule(s)? Like liking like! *RSC Adv.* **2016**, *6*, 19098−19110.

(9) Varadwaj, P.; Varadwaj, A.; Marques, H.; Yamashita, K. Can Combined Electrostatic and Polarization Effects Alone Explain the F···F Negative-Negative Bonding in Simple Fluoro-Substituted Benzene Derivatives? A First-Principles Perspective. *Computation* **2018**, *6*, 51−84.

(10) Metrangolo, P.; Murray, J. S.; Pilati, T.; Politzer, P.; Resnati, G.; Terraneo, G. The fluorine atom as a halogen bond donor, viz. a positive site. *CrystEngComm* **2011**, *13*, 6593−6596.

(11) Politzer, P.; Murray, J. S.; Clark, T. Halogen bonding and other sigma-hole interactions: a perspective. *Phys. Chem. Chem. Phys.* **2013**, *15*, 11178−11189.

(12) Politzer, P.; Murray, J. S. Halogen bonding: an interim discussion. *ChemPhysChem* **2013**, *14*, 278−294.

(13) Ibrahim, M. A. A.; Hasb, A. A. M. Polarization plays the key role in halogen bonding: a point-of-charge-based quantum mechanical study. *Theor. Chem. Acc.* **2019**, *138*, No. 2.

(14) Johansson, M. P.; Swart, M. Intramolecular halogen-halogen bonds? *Phys. Chem. Chem. Phys.* **2013**, *15*, 11543−11553.

(15) Varadwaj, P. R.; Varadwaj, A.; Jin, B.-Y. Unusual bonding modes of perfluorobenzene in its polymeric (dimeric, trimeric and tetrameric) forms: entirely negative fluorine interacting cooperatively with entirely negative fluorine. *Phys. Chem. Chem. Phys.* **2015**, *17*, 31624−31645.

(16) Pedireddi, V. R.; Reddy, D. S.; Goud, B. S.; Craig, D. C.; Rae, A. D.; Desiraju, G. R. The Nature of Halogen-Center-Dot-Center-Dot-Center-Dot-Halogen Interactions and the Crystal-Structure of 1,3,5,7-Tetraiodoadamantane. *J. Chem. Soc. Perkin Trans. 2* **1994**, *11*, 2353−2360.

(17) Awwadi, F. F.; Willett, R. D.; Peterson, K. A.; Twamley, B. The Nature of Halogen···Halogen Synthons: Crystallographic and Theoretical Studies. *Chem. − Eur. J.* **2006**, *12*, 8952−8960.

(18) Desiraju, G. R.; Parthasarathy, R. The nature of halogen.-cntdot..cntdot..cntdot.halogen interactions: are short halogen contacts due to specific attractive forces or due to close packing of nonspherical atoms? *J. Am. Chem. Soc.* **1989**, *111*, 8725−8726.

(19) Sarma, J. A. R. P.; Desiraju, G. R. The role of Cl.cntdot..cntdot..cntdot.Cl and C-H.cntdot..cntdot..cntdot.O interactions in the crystal engineering of 4-.ANG. short-axis structures. *Acc. Chem. Res.* **1986**, *19*, 222−228.

(20) Bent, H. A. Structural Chemistry of Donor-Acceptor Interactions. *Chem. Rev.* **1968**, *68*, 587−648.

(21) Saha, A.; Rather, S. A.; Sharada, D.; Saha, B. K. C−X···X−C vs C−H···X−C, Which One Is the More Dominant Interaction in Crystal Packing (X = Halogen)? *Cryst. Growth Des.* **2018**, *18*, 6084−6090.

(22) Bui, T. T. T.; Dahaoui, S.; Lecomte, C.; Desiraju, G. R.; Espinosa, E. The Nature of Halogen···Halogen Interactions: A Model Derived from Experimental Charge-Density Analysis. *Angew. Chem., Int. Ed.* **2009**, *48*, 3838−3841.

(23) Varadwaj, A.; Marques, H. M.; Varadwaj, P. R. Is the Fluorine in Molecules Dispersive? Is Molecular Electrostatic Potential a Valid Property to Explore Fluorine-Centered Non-Covalent Interactions? *Molecules* **2019**, *24*, 379−407.

(24) Varadwaj, P. R.; Varadwaj, A.; Marques, H. M. Halogen Bonding: A Halogen-Centered Noncovalent Interaction Yet to Be Understood. *Inorganics* **2019**, *7*, 40−102.

(25) Varadwaj, A.; Varadwaj, P. R.; Yamashita, K. Do surfaces of positive electrostatic potential on different halogen derivatives in molecules attract? like attracting like! *J. Comput. Chem.* **2018**, *39*, 343−350.

(26) Bundhun, A.; Ramasami, P.; Murray, J. S.; Politzer, P. Trends in σ-hole strengths and interactions of F3MX molecules (M = C, Si, Ge and X = F, Cl, Br, I). *J. Mol. Model.* **2013**, *19*, 2739−2746.

(27) Weiner, P. K.; Langridge, R.; Blaney, J. M.; Schaefer, R.; Kollman, P. A. Electrostatic potential molecular surfaces. *Proc. Natl. Acad. Sci. U.S.A.* **1982**, *79*, 3754−3758.

(28) Brinck, T.; Murray, J. S.; Politzer, P. Surface Electrostatic Potentials of Halogenated Methanes as Indicators of Directional Intermolecular Interactions. *Int. J. Quantum Chem.* **1992**, *44*, 57−64.

(29) Auffinger, P.; Hays, F. A.; Westhof, E.; Ho, P. S. Halogen bonds in biological molecules. *Proc. Natl. Acad. Sci. U.S.A.* **2004**, *101*, 16789−16794.

(30) Bader, R. F. W. Atoms in Molecules. *Acc. Chem. Res.* **1985**, *18*, 9−15.

(31) Lao, K. U.; Herbert, J. M. Energy Decomposition Analysis with a Stable Charge-Transfer Term for Interpreting Intermolecular Interactions. *J. Chem. Theory Comput.* **2016**, *12*, 2569−2582.

(32) Møller, C.; Plesset, M. S. Note on an Approximation Treatment for Many-Electron Systems. *Phys. Rev.* **1934**, *46*, 618−622.

(33) Woon, D. E.; Dunning, T. H. Gaussian basis sets for use in correlated molecular calculations. IV. Calculation of static electrical response properties. *J. Chem. Phys.* **1994**, *100*, 2975−2988.

(34) Woon, D. E.; Dunning, T. H. Gaussian basis sets for use in correlated molecular calculations. III. The atoms aluminum through argon. *J. Chem. Phys.* **1993**, *98*, 1358−1371.
(35) Feller, D. The role of databases in support of computational chemistry calculations. *J. Comput. Chem.* **1996**, *17*, 1571−1586.
(36) Ibrahim, M. A. A. Molecular mechanical perspective on halogen bonding. *J. Mol. Model.* **2012**, *18*, 4625−4638.
(37) Lu, T.; Chen, F. Multiwfn: a multifunctional wavefunction analyzer. *J. Comput. Chem.* **2012**, *33*, 580−592.
(38) Ibrahim, M. A. A.; Moussa, N. A. M.; Safy, M. E. A. Quantum-mechanical investigation of tetrel bond characteristics based on the point-of-charge (PoC) approach. *J. Mol. Model.* **2018**, *24*, No. 219.
(39) Ibrahim, M. A. A.; Safy, M. E. A. A new insight for chalcogen bonding based on Point-of-Charge approach. *Phosphorus, Sulfur Silicon Relat. Elem.* **2019**, *194*, 444−454.
(40) Ibrahim, M. A. A.; Telb, E. M. Z. A Computational Investigation of Unconventional Lone-Pair Hole Interactions of Group V−VIII Elements. *ChemistrySelect* **2019**, *4*, 5489−5495.
(41) Ibrahim, M. A. A.; Mahmoud, A. H. M.; Moussa, N. A. M. Comparative investigation of $\pm\sigma$−hole interactions of carbon-containing molecules with Lewis bases, acids and di-halogens. *Chem. Pap.* **2020**, *74*, 3569−3580.
(42) Ibrahim, M. A. A.; Hasb, A. A. M.; Mekhemer, G. A. H. Role and nature of halogen bonding in inhibitor···receptor complexes for drug discovery: casein kinase-2 (CK2) inhibition as a case study. *Theor. Chem. Acc.* **2018**, *137*, No. 38.
(43) Ibrahim, M. A. A.; Ahmed, O. A. M.; Moussa, N. A. M.; El-Taher, S.; Moustafa, H. Comparative investigation of interactions of hydrogen, halogen and tetrel bond donors with electron-rich and electron-deficient π-systems. *RSC Adv.* **2019**, *9*, 32811−32820.
(44) Boys, S. F.; Bernardi, F. The calculation of small molecular interactions by the differences of separate total energies. Some procedures with reduced errors. *Mol. Phys.* **1970**, *19*, 553−566.
(45) Mishra, B. K.; Karthikeyan, S.; Ramanathan, V. Tuning the C-H...pi Interaction by Different Substitutions in Benzene-Acetylene Complexes. *J. Chem. Theory Comput.* **2012**, *8*, 1935−1942.
(46) Johnson, E. R.; Keinan, S.; Mori-Sánchez, P.; Contreras-García, J.; Cohen, A. J.; Yang, W. Revealing Noncovalent Interactions. *J. Am. Chem. Soc.* **2010**, *132*, 6498−6506.
(47) Hohenstein, E. G.; Parrish, R. M.; Sherrill, C. D.; Turney, J. M.; Schaefer, H. F., 3rd Large-scale symmetry-adapted perturbation theory computations via density fitting and Laplace transformation techniques: investigating the fundamental forces of DNA-intercalator interactions. *J. Chem. Phys.* **2011**, *135*, 174107−174119.
(48) Hohenstein, E. G.; Sherrill, C. D. Density fitting and Cholesky decomposition approximations in symmetry-adapted perturbation theory: Implementation and application to probe the nature of pi-pi interactions in linear acenes. *J. Chem. Phys.* **2010**, *132*, 184111−184120.
(49) Turney, J. M.; Simmonett, A. C.; Parrish, R. M.; Hohenstein, E. G.; Evangelista, F. A.; Fermann, J. T.; Mintz, B. J.; Burns, L. A.; Wilke, J. J.; Abrams, M. L.; Russ, N. J.; Leininger, M. L.; Janssen, C. L.; Seidl, E. T.; Allen, W. D.; Schaefer, H. F.; King, R. A.; Valeev, E. F.; Sherrill, C. D.; Crawford, T. D. PSI4: an open-source ab initio electronic structure program. *Wiley Interdiscip. Rev.: Comput. Mol. Sci.* **2012**, *2*, 556−565.
(50) Frisch, M. J.; Trucks, G. W.; Schlegel, H. B.; Scuseria, G. E.; Robb, M. A.; Cheeseman, J. R.; Scalmani, G.; Barone, V.; Mennucci, B.; Petersson, G. A.; Nakatsuji, H.; Caricato, M.; Li, X.; Hratchian, H. P.; Izmaylov, A. F.; Bloino, J.; Zheng, G.; Sonnenberg, J. L.; Hada, M.; Ehara, M.; Toyota, K.; Fukuda, R.; Hasegawa, J.; Ishida, M.; Nakajima, T.; Honda, Y.; Kitao, O.; Nakai, H.; Vreven, T.; Montgomery, J. A.; Peralta, J. E.; Ogliaro, F.; Bearpark, M.; Heyd, J. J.; Brothers, E.; Kudin, K. N.; Staroverov, V. N.; Kobayashi, R.; Normand, J.; Raghavachari, K.; Rendell, A.; Burant, J. C.; Iyengar, S. S.; Tomasi, J.; Cossi, M.; Rega, N.; Millam, J. M.; Klene, M.; Knox, J. E.; Cross, J. B.; Bakken, V.; Adamo, C.; Jaramillo, J.; Gomperts, R.; Stratmann, R. E.; Yazyev, O.; Austin, A. J.; Cammi, R.; Pomelli, C.; Ochterski, J. W.; Martin, R. L.; Morokuma, K.; Zakrzewski, V. G.; Voth, G. A.; Salvador, P.; Dannenberg, J. J.; Dapprich, S.; Daniels, A. D.; Farkas, Ö.; Foresman, J. B.; Ortiz, J. V.; Cioslowski, J.; Fox, D. J. *Gaussian 09*, revision E01; Gaussian Inc.: Wallingford, CT, USA, 2009.
(51) Humphrey, W.; Dalke, A.; Schulten, K. VMD: visual molecular dynamics. *J. Mol. Graphics* **1996**, *14*, 33−38.
(52) Groom, C. R.; Bruno, I. J.; Lightfoot, M. P.; Ward, S. C. The Cambridge Structural Database. *Acta Crystallogr., Sect. B: Struct. Sci., Cryst. Eng. Mater.* **2016**, *72*, 171−179.
(53) Allen, F. H. The Cambridge Structural Database: a quarter of a million crystal structures and rising. *Acta Crystallogr., Sect. B: Struct. Sci.* **2002**, *58*, 380−388.

https://dx.doi.org/10.1021/acsomega.0c02887
ACS Omega 2020, 5, 21824−21835